https://doi.org/10.5194/ms-2026-167
Preprint. Discussion started: 7 September 2026

mechanical sciences
DISCUSSIONS

Mechanism-Structure Collaborative Optimization Design of Excavator Stick under Hard-Soil Conditions

Kaitao Ren[1], Zhigui Ren[1,2], Heng Zhang[1], Yijian Zhang[1], Yuxiang Chen[1], Ruibo Liu[1]

1Department of Mechanical Engineering, Shaanxi University of Technology, Hanzhong 723000, China

2Key Laboratory of Industrial Automation, Shaanxi University of Technology, Hanzhong 723001, China.

Correspondence to: Zhigui Ren / zguiren2014@163.com

Abstract: During dense hard-soil excavation, the stick sustains large digging resistance, and long-term static and cyclic impact loads frequently cause failure of critical structural components. Balancing structural performance and digging capacity remains a core bottleneck in excavator attachment design. Using a 20-ton hydraulic excavator as the research prototype, this study proposes a Structure-Mechanism Collaborative Optimization (CO) approach that explicitly accounts for the coupling between mechanism parameters and structural performance. A multidisciplinary CO model was constructed, in which stick digging force and equivalent von Mises stress were calculated from experimental data and critical dangerous conditions were identified from stress distributions. Optimal Latin Hypercube Design (OLHD) combined with Kriging surrogate models was employed to build three surrogate models for digging force, maximum equivalent stress, and stick mass, substantially reducing computational cost. The CO model was subsequently solved by intelligent optimization algorithms under practical engineering constraints. Results demonstrate a 9% increase in theoretical digging force, a 7% reduction in maximum equivalent stress, and a 9% decrease in stick weight.

Keywords: Stick, Collaborative Optimization, Parametric model, Surrogate Model

Introduction

Hydraulic excavators are widely used in civil engineering, mining, water conservancy, and transportation, where operational performance and structural reliability directly affect construction efficiency and project costs. The working mechanism, as the core executive component, endures complex alternating loads. During hard-soil excavation, the stick bears heavy loads and substantial resistance under long-duration impacts, creating high damage risks for critical components. Achieving higher digging force, improved structural integrity, and a shorter design cycle remains a key challenge in excavator mechanism design.

With advances in CAD, FEA, and numerical optimization, simulation-driven design has become mainstream in construction machinery research. Bucket-soil interaction studies provide theoretical support for excavation performance evaluation (Blouin et al., 2001; Maciejewski et al., 2003). Tao et al. (2025) applied an improved mayfly algorithm to stick size optimization, simultaneously achieving lightweighting and performance gains. Liu et al. (2025) proposed a machine-learning-based hierarchical framework for component optimization and fatigue reliability assessment, improving efficiency over traditional methods. Mohan et al. (2024) used FEA and topology optimization on bucket teeth to reduce weight while preserving strength. Li (2017) combined improved PSO with Kriging surrogates for working-mechanism optimization, substantially cutting computational cost. Zu and Bai (2025) developed a BIM-driven optimization model integrating grid-search and immune genetic algorithms to enhance global search capability. Alaei et al. (2019) presented a product development methodology for mobile machinery

https://doi.org/10.5194/ms-2026-167
Preprint. Discussion started: 7 September 2026

mechanical sciences
DISCUSSIONS

using an excavator case study.

Structural optimization of working attachments has been extensively studied (Wu & Cai, 2026; Chang et al., 2024; Huang et al., 2025; Yu et al., 2019; Li et al., 2014). Solazzi et al. (2019, 2021, 2022) con aducted numerical-experimental studies and fatigue assessment on composite booms, showing that alternating loads significantly degrade fatigue safety margins. NSGA-II has been widely adopted for complex multi-objective engineering design (Deb et al., 2002). Zhou and Wang (2022) coupled surrogate models with adaptive simulated annealing for boom-stick lightweighting. Qiu et al. (2016) compared surrogate model performance and built a multi-surrogate framework for working attachments. Kim et al. (2014) optimized front linkage hinge-point coordinates to improve digging capacity. Zhang et al. (2024) used a 500-point surrogate model with genetic algorithms for boom optimization. Wu et al. (2024) proposed a BLISCO-embedded collaborative optimization method for electric shovel design, demonstrating reduced excavation resistance and improved structural safety. Lu et al. (2023) established an energy-oriented multi-objective collaborative optimization model outperforming conventional strategies.

Despite these advances, key limitations remain. Most studies optimize single components or independent parameters, ignoring coupling between structural plate and mechanism hinge parameters, with limited focus on hard-soil conditions. Three bottlenecks persist under compacted hard-soil excavation: insufficient cutting thrust, high equivalent stress from persistent impact loads, and lengthy optimization cycles—necessitating targeted multi-objective stick optimization research.

To address the above limitations, this study adopts a collaborative optimization framework and develops a mechanism-structural CO model for the excavator stick to capture coupling effects between structural and mechanism parameters of the working attachment. Experimental excavation data of a 20-ton hydraulic excavator under hard-soil conditions are collected to establish its parametric model. Based on D'Alembert's equilibrium equations and the stick digging-force model, extreme digging forces and structural loads along the target trajectory are calculated to identify hazardous working conditions for optimization. To reduce computational cost and shorten the design cycle, Kriging surrogate models for digging force, maximum stress and stick self-weight are established. The CO model is finally solved, and the overall research framework is presented in Fig. 1.

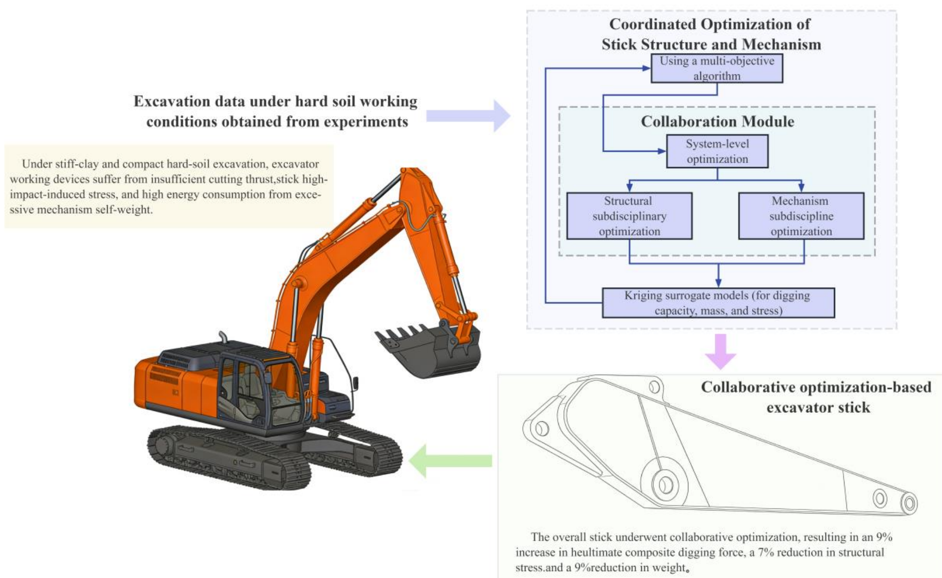

Figure 1. Framework diagram for excavator collaborative optimization.Optimization solution process

https://doi.org/10.5194/ms-2026-167
Preprint. Discussion started: 7 September 2026

1 Load Case Analysis

1.1 Acquisition of load data

This study used a 20-metric-ton backhoe hydraulic excavator as the test prototype. Through experiments, excavation trajectories and hydraulic pressure data were acquired at different excavation depths (ground surface, 1 m, and 2 m) under hard soil conditions. These three depths correspond to light-load topsoil cutting, medium-load conventional excavation, and heavy-load deep excavation working conditions, respectively. The test conditions cover the typical operating range of the excavator, facilitating a systematic analysis of load characteristics under various soil failure modes. Fig 2 illustrates the experimental excavation process. Fig 3 shows the data acquisition platform adopted in this experiment.

Figure 2. Excavation test process.

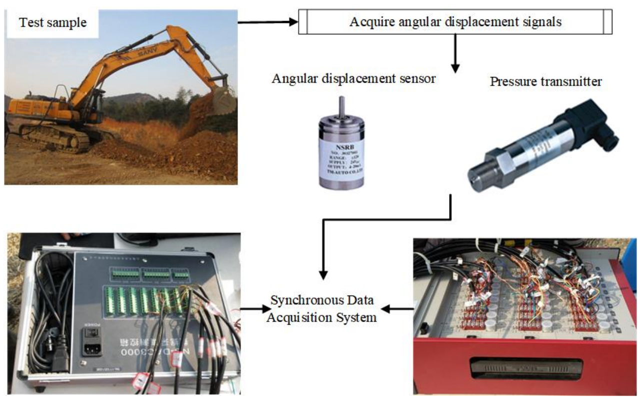

Figure 3. Integrated experimental test platform.

Hydraulic pressure data of each excavator cylinder under compacted hard soil at different digging depths were acquired via field experiments, as plotted in Fig 4.

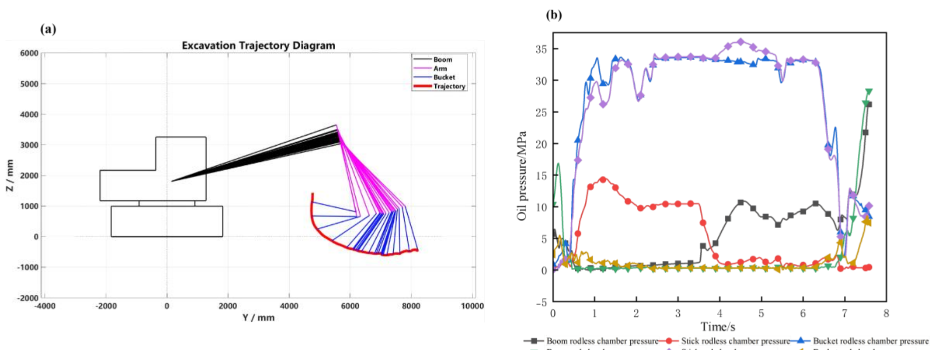

https://doi.org/10.5194/ms-2026-167
Preprint. Discussion started: 7 September 2026

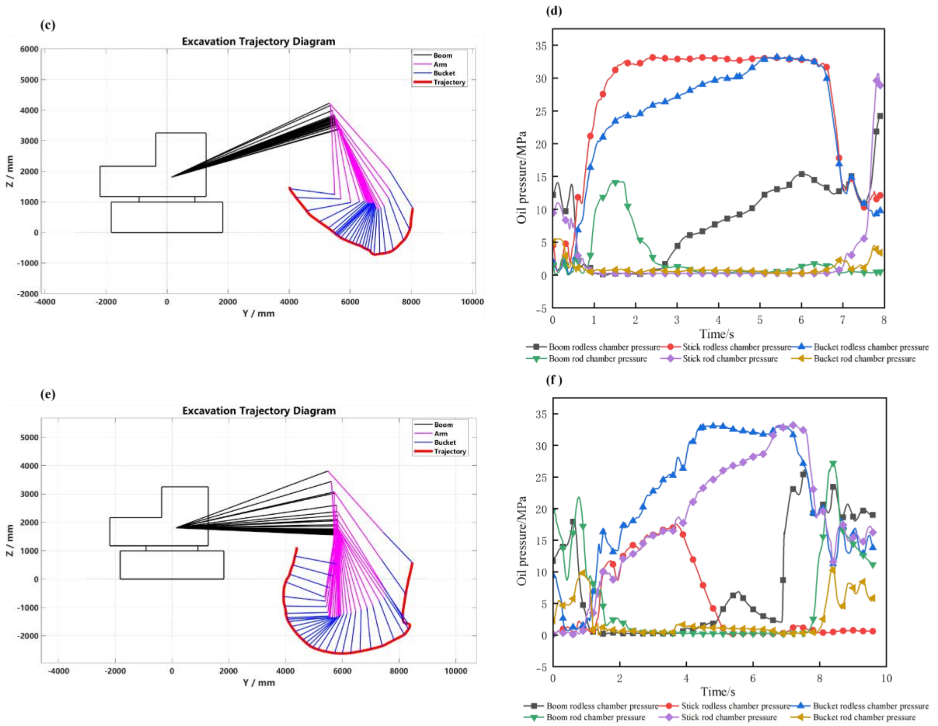

Figure 4. Measured oil pressure data under different excavation depths: (a) Surface digging trajectory; (b) Measured hydraulic pressure (surface trajectory); (c) 1 m digging trajectory; (d) Measured hydraulic pressure (1 m surface trajectory); (e) 2 m digging trajectory; (f) Measured hydraulic pressure (2 m surface trajectory).

The excavation trajectory at 1 m digging depth had a short travel range. The bucket rapidly penetrated compacted hard soil during primary cutting, concentrating resistance loads and producing a prominent impact effect. Thus, the 1 m condition was selected for subsequent analysis. Conventional resistance calculation relies on passive soil mechanical models, requiring complex soil parameters (e.g., cohesion, internal friction angle) and intricate nonlinear tool-soil contact boundaries, limiting accuracy under variable field conditions. The active-side method for normal incomplete excavation resistance proposed by Ren et al. (2019) avoids these dependencies, solving resistance solely from measured active-side motion parameters and cylinder pressure data. Using this measured data, the excavation resistance for the composite trajectory was calculated.

The load-geometry relationship is visualized by mapping back-calculated digging resistance to corresponding bucket-tip trajectory points via forward mechanism solutions, yielding the spatial distribution scatter plot in Fig 5. Structural failure and fatigue damage in heavy machinery components (e.g., sticks, booms) typically occur during critical stages with extreme load surges or sustained high stress. Analyzing light-load or no-load conditions would cause redundant computation and overly conservative designs. Therefore, boundary extraction was applied to the highest-load interval in Fig 5, isolating the core segment AB bearing peak resistance and intense load fluctuations. This segment serves as the core dynamic boundary condition for subsequent collaborative optimization of the stick structure and mechanism.

https://doi.org/10.5194/ms-2026-167
Preprint. Discussion started: 7 September 2026

mechanical sciences
DISCUSSIONS

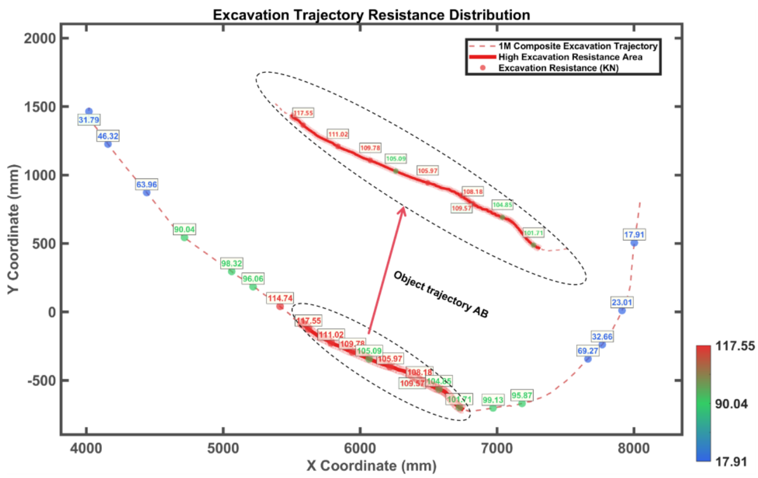

Figure 5. Excavation trajectory and resistance distribution map.

Based on the trajectory and oil-pressure data measured in the above-mentioned experiments, the corresponding stick digging force for segment AB can be calculated. Fig 6 shows the time-history curve of the stick digging force along segment AB. The measured maximum digging force in this segment reaches 105.165 kN during the test.

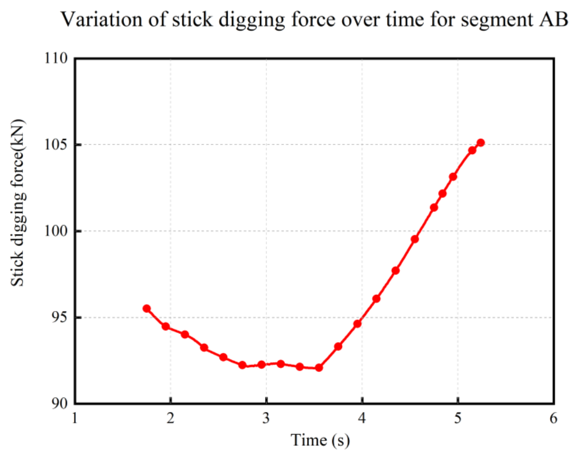

Figure 6. Schematic diagram of digging force in segment AB.

1.2 Structural analysis

The stick serves as the critical working component of the backhoe hydraulic excavator's operating mechanism. To facilitate model preservation, repeated model retrieval and analysis during the process, as well as subsequent calculation of sample point Stick quality, this study employs APDL language to establish a parametric model of the excavator's operating mechanism and conducts finite element analysis on the mechanism. Command streams are utilized to assign values for the Stick's structural parameters, mesh element types, material parameters, and load parameters for calculation. Parametric modelling of the working device necessitates simplification by omitting minor details. The complete command stream is ultimately saved as a macro file for convenient subsequent analysis and optimization calls. The parametric model is illustrated in Fig 7 (a).

https://doi.org/10.5194/ms-2026-167
Preprint. Discussion started: 7 September 2026

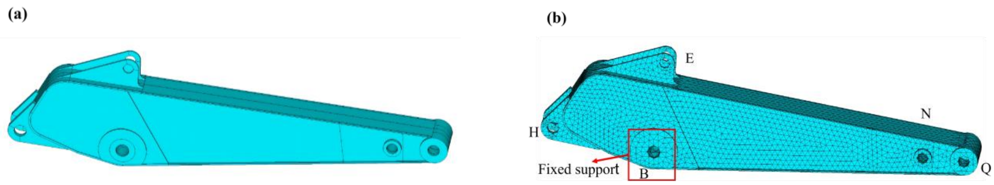

Figure 7. Parametric model and meshing of the stick: (a) Parametric model of the stick; (b) Grid partitioning.

Table 1. Material properties

Material	Elastic modulus E (GPa)	Density ρ (kg·m^3)	Poisson's ratio ν	Yield strength σ_s (GPa)
Q345	206	7850	0.3	345

All working components of the 20-ton excavator are made of Q345 steel, whose material properties are given in Table 1. As shown in Fig. 7(b), the finite-element model is meshed with high-order three-dimensional SOLID187 solid elements. This element contains ten nodes, and each node has translational degrees of freedom in the x, y and z directions. Equipped with mid-side nodes, the SOLID187 element can represent the geometric features of the structure with high precision. For subsequent analyses, hinge point B is defined as the fixed-support boundary condition, and forces are applied to the other four hinge points.

Hinge-point force distribution for excavator working equipment is complex, and load-application methods greatly influence structural-analysis results. In reality, pin-connected hinges experience loads distributed over a specific angular range on the pin-hole cylindrical surface, instead of single-point concentrated loads. Concentrated point loads and uniformly distributed loads cannot replicate actual loading behaviours and produce artificial local stress concentrations. This study adopts a cosine-distributed load scheme to accurately simulate real loading at hinge bores and eliminate spurious stress concentrations. APDL automates force application for each hinge point of the stick, as shown in Fig. 8.

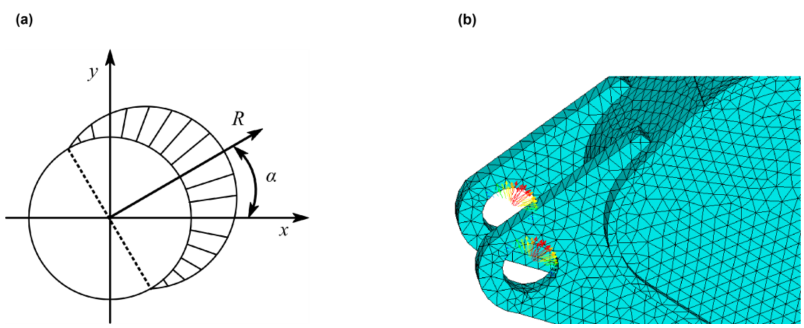

Figure 8. Cosine load assumed distribution diagram and distribution application schematic: (a) Cosine load assumed distribution diagram; (b) Distribution application schematic.

With D'Alembert's equilibrium equations and acquired excavation-resistance data of segment AB, static-equivalent dynamic loads of the stick mechanism are solved. Considering component inertial forces and moments, mechanism force-balance analysis computes resultant hinge-point loads for the four hinges excluding fixed-support hinge point B (Fig. 9(a)). These resultant hinge-point forces are imposed as external boundary conditions on the stick finite-element model. Transient stress

https://doi.org/10.5194/ms-2026-167
Preprint. Discussion started: 7 September 2026

simulation under the aforementioned load-application scheme yields the time-history stress-response curve of the stick for segment AB (Fig. 9(b)). The maximum stick stress occurs at 4.73 s; this condition is defined as the hazardous working condition for subsequent structural optimization.

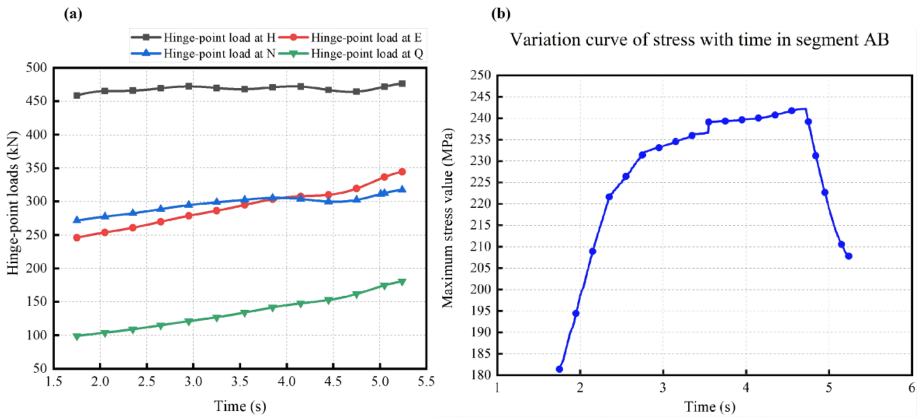

Figure 9. Load diagram and stress diagram: (a) hinge-point load diagram; (b) Time-history stress diagram.

2 Establishing a surrogate model based on kriging

The primary fabrication of the components of an excavator's working device is by welding steel plates, with the result that the Stick features complex structural configurations. This means that a single finite element analysis calculation for the Stick consumes significant computational time. In order to reduce these costs and shorten the subsequent collaborative optimization iteration cycle, this study employs a surrogate model to establish a mapping relationship between design variables and responses based on sample data (Han et al., 2012).

Optimal Latin Hypercube Design (OLHD) produced 300 sample points to build the Kriging surrogate model. Among these samples, 240 were used as training data for model fitting to evaluate prediction accuracy and generalization performance, and the remaining 60 independent samples acted as test data to verify model precision. Comparison of the proxy model's prediction results with finite element calculation results demonstrates that the model exhibits high prediction accuracy and good generalization capability at this sample size, thus confirming the appropriateness of the selected number of sample points.

Fig 10 presents comparison curves and scatter plots between predicted and actual values of stress, mass and digging force for sample points in the training and test sets of the Kriging surrogate model. The root-mean-square error (RMSE) and coefficient of determination R^2 of each surrogate model on both training and test sets are also provided. Most sample points of the three surrogate models lie close to the 45° diagonal line, and the deviation levels of the training set are similar to those of the test set. In addition, the R^2 values of each surrogate model are close to 0.9 for both the training and test sets. These results demonstrate that the constructed surrogate models achieve high fitting accuracy, favorable prediction capability and satisfactory generalization performance. Accordingly, the surrogate models can be directly adopted in optimization calculations, which greatly improves computational efficiency.

https://doi.org/10.5194/ms-2026-167
Preprint. Discussion started: 7 September 2026

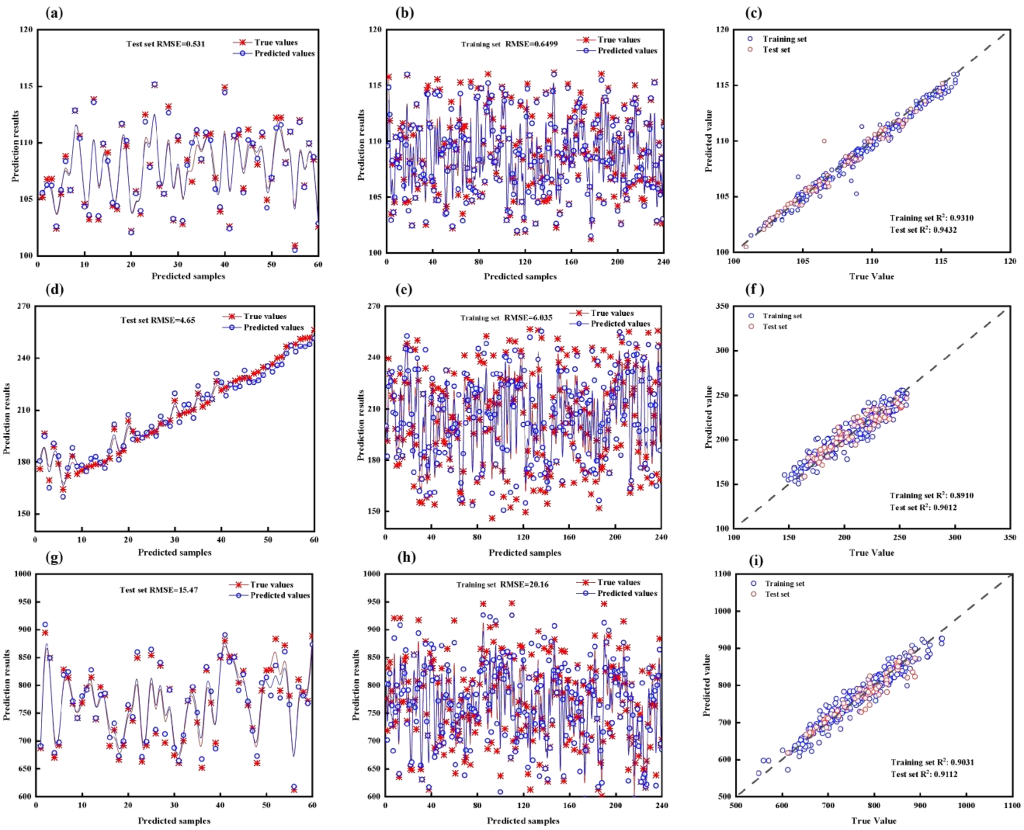

Figure 10. Experimental design and surrogate model: (a) Test-set actual-predicted digging-force comparison curve; (b) Training-set actual-predicted digging-force comparison curve; (c) Predicted-versus-actual digging-force scatter plot; (d) Test-set actual-predicted stress comparison curve; (e) Training-set actual-predicted stress comparison curve; (f) Predicted-versus-actual stress scatter plot; (g) Test-set actual-predicted mass comparison curve; (h) Training-set actual-predicted mass comparison curve; (i) Predicted-versus-actual mass scatter plot.

3 Mechanism-structure collaborative optimization model

The working mechanism of excavators forms a complex engineering system, whose design corresponds to an inherent multidisciplinary coupled optimization problem. Complex data exchange and physical coupling occur across subsystems from different disciplines. Conventional serial or separate optimization methods cannot effectively resolve multidisciplinary conflicts and tend to converge to local optima. To solve the coupling problems between structural performance and mechanical motion, this study adopts the collaborative optimization (CO) method.

Collaborative Optimization (CO) was originally proposed by Kroo et al. (1994) from Stanford University in 1994. Featuring clear disciplinary independence and a two-level hierarchical framework, the CO method is theoretically suitable for multidisciplinary optimization problems with coupled Mechanism-Structural variables. Targeting the aforementioned multidisciplinary coupling optimization characteristics of excavator working mechanisms, this paper applies the core principles of CO to carry out structure-mechanism collaborative optimization research on excavator sticks. The complete structure-mechanism collaborative optimization framework is presented in Fig 11.

https://doi.org/10.5194/ms-2026-167
Preprint. Discussion started: 7 September 2026

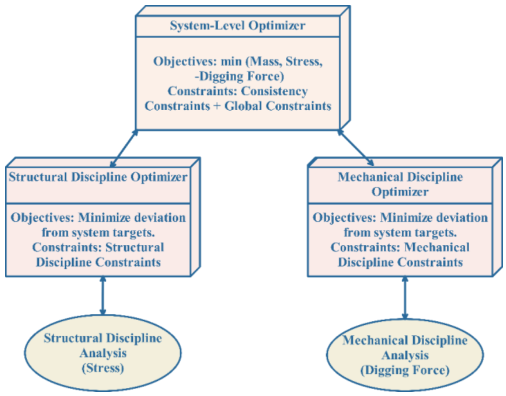

Figure 11. Classic collaborative optimization framework diagram.

3.1 Determination of design variables

Structural design variables include plate thicknesses and key dimensional parameters that greatly affect the equivalent stress and self-weight of the working attachment. Mechanism design variables are defined as the distances and included angles between each hinge point of the stick. Table 2 lists the stick structural design variables together with their constraint ranges. All plate-thickness variables are bounded between 0.5 and 1.5 times their baseline design values, while spacing parameters are restricted within 0.8–1.2 times their baseline dimensions. Table 3 sizes the mechanism design variables and their corresponding constraint ranges, where distances and included angles are also limited to 0.8–1.2 times their baseline dimensions. The schematic diagram of structural and mechanism parameters is shown in Fig 12.

Table 2 Structural design variables and constraints.

No.	Name	Code name	Constraint
1	Distance between stick side plates	x_{s1}/mm	$188 < x_{s1} < 280$
2	Thickness of the stick rear side plate	x_{s2}/mm	$8 < x_{s2} < 24$
3	Thickness of the stick cylinder hinge ear plate	x_{s3}/mm	$15 < x_{s3} < 45$
4	Thickness of Bucket cylinder hinge ear plate	x_{s4}/mm	$16 < x_{s4} < 46$
5	Thickness of the stick front side plate	x_{s5}/mm	$8 < x_{s5} < 24$
6	Thickness of the stick middle side plate	x_{s6}/mm	$5 < x_{s6} < 15$
7	Thickness of the stick front top plate	x_{s7}/mm	$7 < x_{s7} < 21$
8	Thickness of the Stick rear top plate	x_{s8}/mm	$7 < x_{s8} < 21$
9	Thickness of the stick cylinder hinge bend plate	x_{s9}/mm	$8 < x_{s9} < 24$
10	Thickness of the stick bottom plate	x_{s10}/mm	$10 < x_{s10} < 30$

Table 3 Mechanism design variables and constraints.

No.	Name	Code name	Constraint
1	Length between hinge points BQ	x_{k1}/mm	$2769 < x_{k1} < 3061$
2	Length between hinge points BH	x_{k2}/mm	$807 < x_{k2} < 893$
3	Length between hinge points BE	x_{k3}/mm	$631 < x_{k3} < 698$
4	Length between hinge points BN	x_{k4}/mm	$2380 < x_{k4} < 2631$
5	Angle formed by the three-point connection of hinge points QBH	x_{k5}/°	$156 < x_{k5} < 172$
6	Angle formed by the three-point connection of hinge points QBE	x_{k6}/°	$70 < x_{k6} < 80$
7	Angle formed by the three-point connection of hinge points QBN	x_{k7}/°	$0.3 < x_{k7} < 1.5$

https://doi.org/10.5194/ms-2026-167
Preprint. Discussion started: 7 September 2026

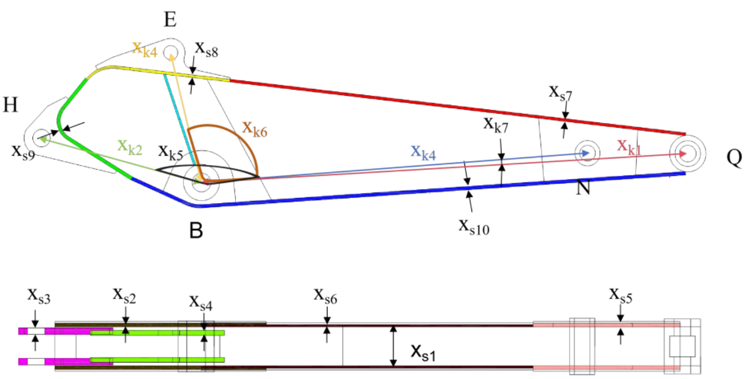

Figure 12. Schematic of mechanism and structural parameters.

The structural design variables mentioned above are denoted as $x_s = [x_{s1}, x_{s2}, \ldots, x_{s10,}]^T$; mechanism discipline design variables are denoted as $x_k = [x_{k1}, x_{k2}, \ldots, x_{k7,}]^T$. Within the Collaborative Optimization framework, a coordination variable is introduced at the system level. Its components share the same physical meaning as the discipline-level design variables, enabling consistent coordination of multidisciplinary design outcomes at the system level. The coordination variable $Z = [Z_s, Z_k]^T$, The constraints for system-level design variables are identical to those for sub-discipline design variables.

3.2 Collaborative optimization framework and mathematical model

This study adopted a consistency-constrained CO framework with a two-tier system-disciplinary architecture to implement multi-objective optimization. The system-level optimization aims to obtain the global optimal solution by coordinating the coupling effects among different disciplines. For excavators operating in harsh hard-soil working conditions with high digging-capacity requirements, stick digging force is taken as Objective 1. The maximum stick stress under critical working conditions, which is constrained within the allowable safety range, is defined as Objective 2. A lightweight working attachment reduces structural inertia and enhances the operational flexibility of excavators, so its total mass is defined as the third optimization objective. These three indicators form the global system-level optimization objectives, which are formulated as follows.

$$
\begin{aligned}
\min \quad & y_1 = -f \\
& y_2 = \sigma_{\max} \\
& y_3 = m
\end{aligned}
\tag{1}
$$

In Eq.(1), f represents the stick digging force; $\sigma_{\max}$ represents the maximum equivalent von Mises stress under hazardous conditions and m represents the stick self-weight.

Collaborative optimization (CO) is a two-level distributed multidisciplinary optimization approach. At the system level, the global multi-objective problem is solved. This level allocates design variables to each sub-discipline and receives design information returned from sub-disciplines. Disciplinary consistency constraints are introduced to coordinate the deviations of coupled variables across sub-disciplines. At the sub-discipline level, constrained local optimization is carried out on surrogate models by taking the design points issued by the system level as references. Design variables satisfying the constraints of the corresponding sub-discipline are acquired, and the optimization results are fed back to the system level. Two-level iterations proceed until the convergence criteria are satisfied.

https://doi.org/10.5194/ms-2026-167
Preprint. Discussion started: 7 September 2026

The system-level optimization model is as follows:

$$\begin{cases} \min F(\mathrm{z}) = \omega_1 \dfrac{y_1}{f_1} + \omega_2 \dfrac{y_2}{[\sigma]} + \omega_3 \dfrac{y_3}{m_1} \\ \text{s.t.} \ -y_1 - f < 0 \\ y_2 - [\sigma] < 0 \\ y_3 - m_1 > 0 \\ \left\| z_i - x_i^* \right\|^2 \le \varepsilon \\ \mathrm{Z}^L < \mathrm{Z} < \mathrm{Z}^U \end{cases} \tag{2}$$

In Equation (1), $[\sigma]$ and m_1 denote the allowable stress and self-weight, respectively; f_1 represents the maximum stick digging force under this excavation condition; $\omega_1, \omega_2, \omega_3$ are weight coefficients that reflect the relative importance of each objective; z_i signifies the expected value of the design variable allocated to the sub-discipline by the system, while x_i^* represents the optimized design variable of the sub-discipline. $i = s$ denotes the structural variable when $i = k$ denotes the structural variable when c represents t represents the mechanism variable; ε enotes the consistency tolerance, a very small positive number; z^L and z^U epresents the upper and lower bounds of the system-level design variables.

Structural Discipline Optimization Model:

As the primary load-bearing component, the structural performance of the hydraulic excavator's Stick directly impacts the overall machine reliability. Structural optimization coordinates design variables at the system level, seeking optimal structural parameters while satisfying stress constraints.

$$\begin{cases} \min J_s(x_s) = \left\| x_s - z_s^* \right\|^2 \\ \text{s.t.} \ \sigma(x_s) - [\sigma] \le 0 \\ x_s^L < x_s < x_s^U \end{cases} \tag{3}$$

In Equation (3), x_s represents the design variable sought for the structural sub-discipline; z_s^* denotes the system's assigned target value for the structural sub-discipline's design variable; $\sigma(x_s)$ indicates the maximum stress corresponding to the optimized design variable of the sub-discipline; σ_1 signifies the maximum stress on the Stick under hazardous conditions; x_s^L and x_s^U denote the upper and lower bounds of the structural design variable.

Mechanism Discipline Optimization Model:

The digging performance of a hydraulic excavator's working equipment is directly determined by its mechanism parameters. Mechanism optimization uses the expected values of system-level allocated mechanism design variables as the coordination benchmark, seeking optimal mechanism parameters while satisfying the theoretical digging force constraint of the Stick cylinder. The optimization mathematical model is as follows:

$$\begin{cases} \min J_k(x_k) = \left\| x_k - \mathrm{z}_k^* \right\|^2 \\ \text{s.t.} \ f(x_k) - f_1 \ge 0 \\ x_k^L < x_k < x_k^U \end{cases} \tag{4}$$

In Equation (4), x_k represents the design variable sought by the sub-discipline mechanism; z_k^* denotes the expected value assigned by the system to the sub-discipline mechanism's design variable; $f(x_k)$ represents the peak stick digging force

https://doi.org/10.5194/ms-2026-167
Preprint. Discussion started: 7 September 2026

mechanical sciences DISCUSSIONS

corresponding to the design variables optimized by the subsystem discipline; x_k^L and x_k^U enote the upper and lower bounds of the structural design variable.

4 Optimizing the solution process

This study developed a CO program in MATLAB, and efficient solutions to the optimization problem can be obtained by selecting a suitable optimization algorithm. The system-level optimization constitutes a high-dimensional multi-objective optimization problem. Accordingly, this study adopted the Nondominated Sorting Genetic Algorithm II (NSGA-II). This algorithm incorporates a fast non-dominated sorting operator, an individual crowding distance operator and an elite selection operator. These features give NSGA-II high computational speed, robust performance and strong global search capabilities. A compromise optimal solution was selected from the obtained Pareto solution set for practical engineering application. For sub-disciplines, the fmincon function in MATLAB is employed and configured in Sequential Quadratic Programming (SQP) mode.

The system transmits the expected values of mechanism and structural design variables to each subdiscipline. Afterwards, the mechanism and structural subdisciplines conduct independent optimization based on the system target values assigned, and feed the optimized local variable sets back to the system level. The system level calculates the discrepancy between the feedback optimized variables and the initially allocated target values, defined as disciplinary inconsistency, and incorporates this inconsistency into the constraint violation degree. The fitness of each individual is evaluated by combining the objective function values predicted by the surrogate models and the disciplinary inconsistency metric. The algorithm then performs genetic operations including selection, crossover and mutation to generate a new population. The above iterative procedures are repeated until the maximum iteration number is reached, yielding a set of Pareto-optimal solutions that achieve the optimal trade-off among multiple conflicting objectives. Fig 13 presents the flowchart of the above solution procedure.

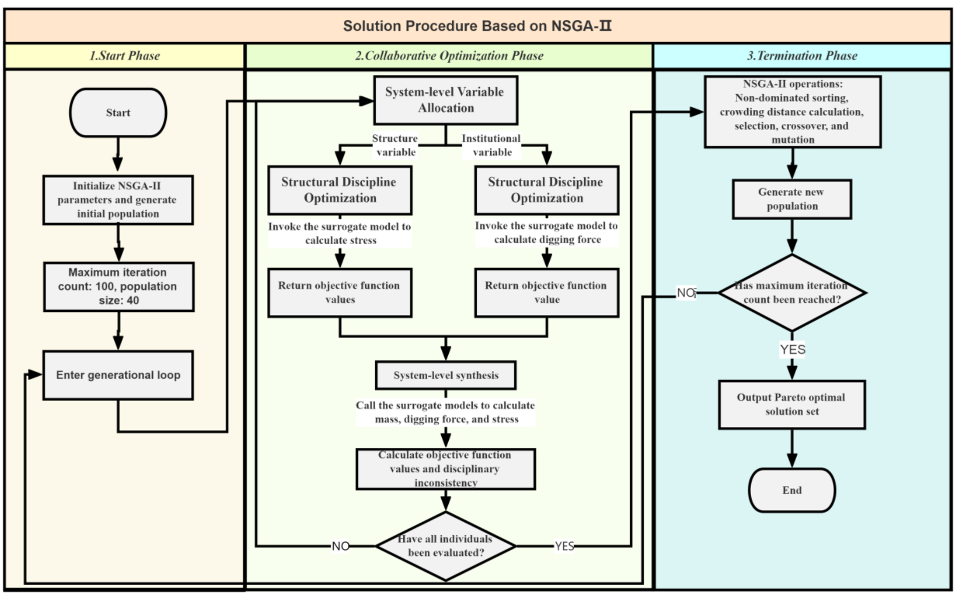

Figure 13. Flowchart of NSGA-II solution process.

https://doi.org/10.5194/ms-2026-167
Preprint. Discussion started: 7 September 2026

mechanical sciences
DISCUSSIONS

5 Analysis of optimization results

Fig 14 shows a set of Pareto-optimal solutions obtained using the NSGA-II genetic algorithm. To obtain a final design satisfying engineering requirements, further multi-objective decision-making analysis is required. Analyses presented in Table 4 were conducted according to the different weight-coefficient combinations defined in Equation (2). For the weight-coefficient combination of $\omega_1 = \omega_1 = 0.4$, $\omega_3 = 0.3$, the design can better satisfy the requirement for improving the stick digging force under hard-soil working conditions while ensuring lower structural stress of the stick. The point marked by the red star in Fig 14 is the compromise optimal solution for this optimization. This compromise optimal solution yields a stick mass of 671.7kg, a maximum von-Mises stress of 227.314 MPa, and a stick digging force of 116.935 kN.

Table 4 Different weight-coefficient combinations.

Item	ω_1	ω_2	ω_3	Stick digging force (kN)	Stick stress (MPa)	Stick mass (t)
Group 1	0.3	0.3	0.3	114.647	236.435	661.3
Group 2	0.2	0.4	0.4	113.965	226.516	676.3
Group 3	0.4	0.4	0.2	116.935	227.314	671.7

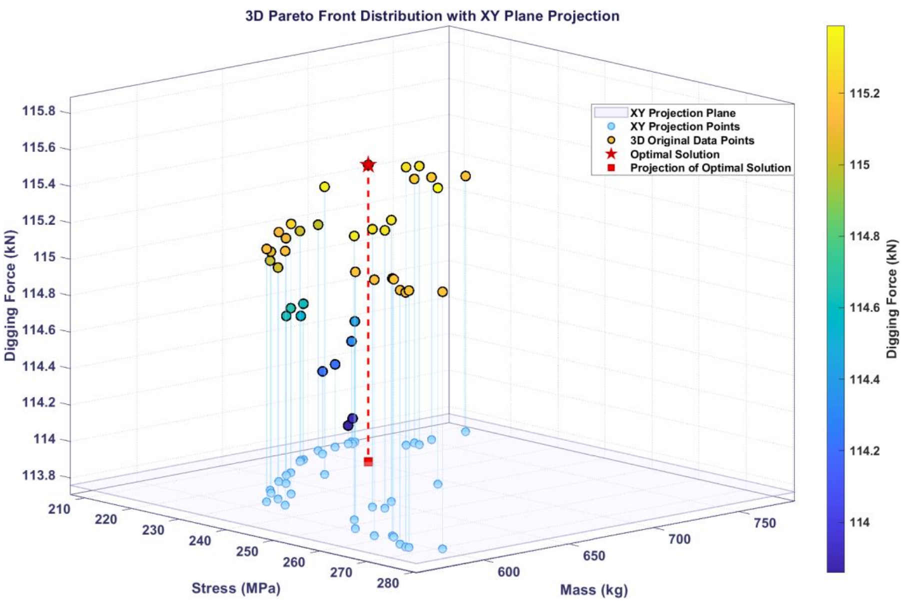

Figure 14. Pareto optimal solution set.

Table 5 lists the structural and mechanism design variables before and after optimization,To verify the reliability of the surrogate-based optimization results, the optimized mechanism and structural parameters were re-imported into the stick digging-force model and the original APDL parametric FEA model for independent re-analysis, As shown in Table 6, the objective values before and after optimization are listed.

The re-calculated values of digging force, maximum equivalent stress, and stick weight were then compared against the surrogate model predictions. The re-analysis results show that the deviations between surrogate predictions and FEA verification

https://doi.org/10.5194/ms-2026-167
Preprint. Discussion started: 7 September 2026

values are 1.368% for digging force, 1.144% for maximum equivalent stress, and 1.414% for stick weight, all remaining within 1.5%. These small discrepancies confirm that the constructed Kriging surrogate models possess sufficient approximation accuracy, and that the collaborative optimization results are physically reliable and engineering-applicable.

Table 5 Comparison before and after design variable optimization.

Structural variables	Before optimization	After optimization	Mechanism variables	Before optimization	After optimization
x_{s1}/mm	234	278.62	x_{k1}/mm	2915	2276.60
x_{s2}/mm	16	17.25	x_{k2}/mm	1050	921.29
x_{s3}/mm	30	44.67	x_{k3}/mm	750	783.64
x_{s4}/mm	31	17	x_{k4}/mm	2506	2408.65
x_{s5}/mm	16	9.25	x_{k5}/°	163. 59	172
x_{s6}/mm	10	7.20	x_{k6}/°	90.1	82.98
x_{s7}/mm	14	7.52	x_{k7}/°	0.61	0.51
x_{s8}/mm	14	10.61			
x_{s9}/mm	16	16.67			
x_{s10}/mm	20	10.30			

Table 6 Comparison of optimization targets before and after.

Project	Stick digging force (kN)	Stick stress (MPa)	Stick mass (kg)
Before optimization	105.165	242.199	750
After optimization	115.385	224.714	681.2
Percentage change	9%	7%	9%

Fig 15 shows the spatial geometric configurations before and after collaborative optimization. The optimized model is more compact, with reduced length and adaptively repositioned hydraulic cylinder hinge points. These adjustments represent a global optimum solved by the CO algorithm to achieve the best force-arm transmission ratio under hard-soil conditions. The repositioned hinges shorten load-bearing lever arms, reduce overall bending moment, and deliver a more compact layout — all while preserving the original digging envelope. As a result, maximum stick digging force increases from 105.165 kN to 115.385 kN (+9%), and total mass decreases from 750 kg to 681.2 kg (−9%).

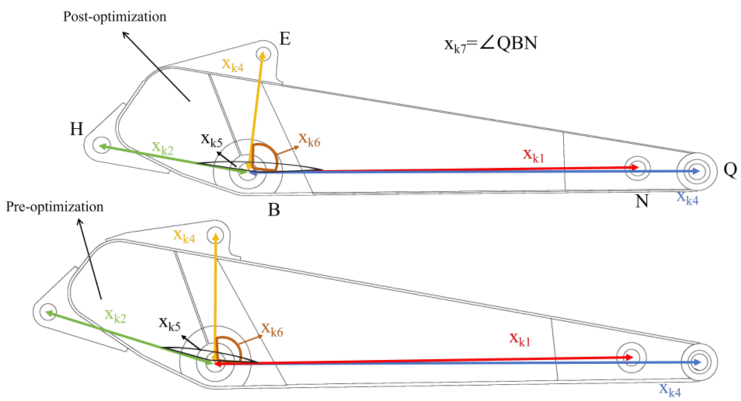

Figure 15. Comparison before and after optimization.

Fig 16 further presents the equivalent stress contours of the stick under the harshest working conditions before and after

https://doi.org/10.5194/ms-2026-167
Preprint. Discussion started: 7 September 2026

optimization. After optimization, the overall stress distribution of the stick exhibits a smoother transition, and a large amount of redundant material subjected to low stress in the original design is removed. Meanwhile, the maximum stress concentration occurs at the welded joint between the bottom plate and side plates in the middle section of the stick, where the component bears the most severe combined bending and torsional loads. Extracted contour data show that the peak equivalent stress in this region reaches 224.714 MPa. Compared with the maximum stress of 242.199 MPa in the initial model, the maximum stress is reduced by 7%, which is considerably lower than the allowable stress (230 MPa) of Q345 high-strength steel. The optimized structure fully satisfies the stiffness and strength design criteria for heavy construction machinery.

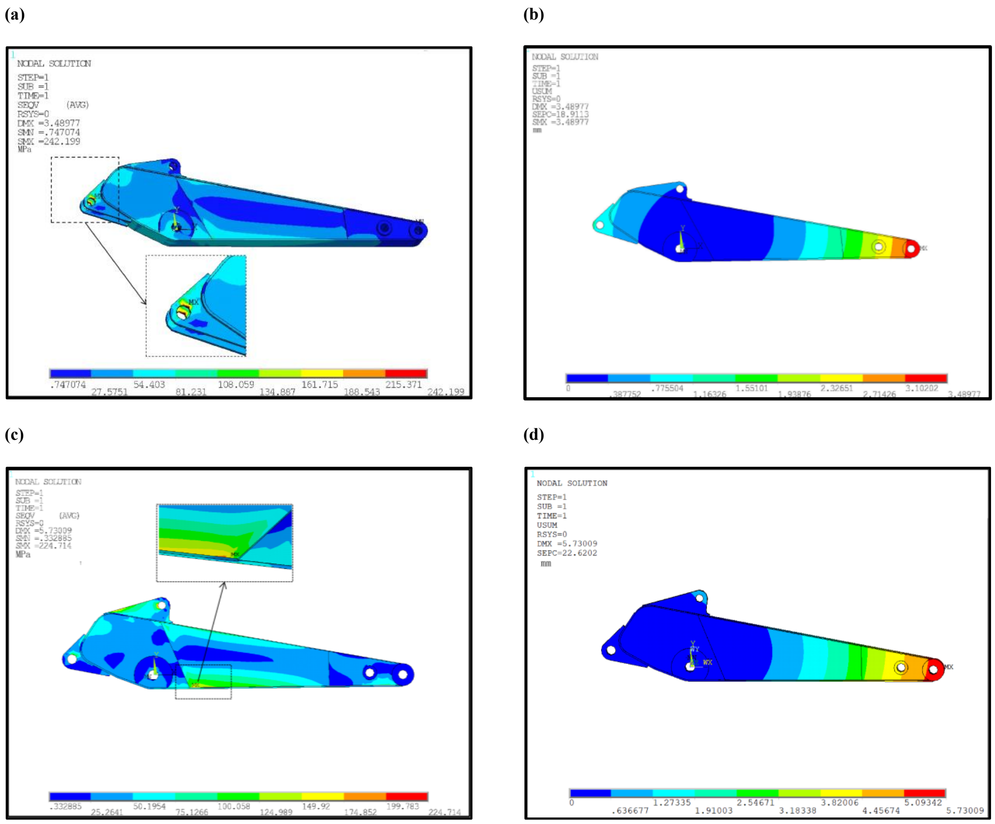

Figure 16. Stress-strain distribution diagram after optimization: (a) Pre-optimization stress contour; (b) Pre-optimization strain contour; (c) Post-optimization stress contour; (d) Post-optimization strain contour

6 Conclusion

This paper addressed two prominent problems of the stick for hydraulic excavators operating in compacted hard soil: insufficient digging capacity and severe stress concentration, along with insufficient consideration of coupling effects between structural and mechanism parameters. Taking a 20-metric-ton-class hydraulic excavator as the research object, this paper proposes a Collaborative Optimization method and carries out multi-objective optimization design for the stick. The main conclusions are as follows:

(1) By analyzing field digging data of a 20-metric-ton excavator under hard soil excavation conditions, the critical working

https://doi.org/10.5194/ms-2026-167
Preprint. Discussion started: 7 September 2026

conditions of the stick under ultimate loads are identified. A multi-response surrogate model relating the stick's digging force, stress and mass is established by means of APDL parametric modeling, optimal Latin hypercube sampling and the Kriging method, which realizes tight coupling of mechanisms and structural mechanics within the multi-objective optimization framework.

(2) The collaborative optimization results demonstrate that the comprehensive performance of the stick is significantly improved. Subject to structural strength and constraint limits, the optimized stick achieves an approximately 9% increase in digging force, a roughly 7% reduction in maximum equivalent stress, and a nearly 9% decrease in mass. The optimization results demonstrate that the proposed method simultaneously achieves a lightweight design and enhanced digging performance without compromising structural safety.

(3) The effectiveness of Mechanism-Structural Collaborative Optimization for hydraulic excavator design is validated. Collaborative Optimization fully considers the coupling effects between mechanism parameters and structural parameters. Via two-level coordination at the system and discipline levels, a Pareto optimal solution more suitable for engineering practice is obtained, which improves design efficiency and overall performance. This work offers a valuable reference for subsequent Multidisciplinary Design Optimization (MDO) of the complete working attachments of hydraulic excavators.

Data availability. The code and data supporting the findings of this study are available from the corresponding author upon rea-sonable request. Access to these data and code is restricted under enterprise confidentiality agreements, which prevent the public release of raw simulation data and parameterised modelling codes. Readers requiring access may contact the corresponding author to request permission.

Author contributions. KR contributed to the conception of the study and funding acquisition. ZR and KR carried out the theoretical analysis. HZ conducted the experiments and drafted the original manuscript. YZ and HN provided technical support for algorithm design. YC and BL summarized the conclusions and took charge of project coordination.

Competing interests. The contact author has declared that none of the authors has any competing interests.

Financial support. This work was supported by the Key Research Program Project of Shaanxi Provincial Department of Science and Technology (No. 2024NC-YBXM-203) and the Shaanxi Provincial Department of Education Service Local Special Industrialization Cultivation Project (No. 24JC024).

https://doi.org/10.5194/ms-2026-167
Preprint. Discussion started: 7 September 2026

Acknowledgments. We sincerely appreciate the valuable contributions from the editor and anonymous reviewers.

References

Alaei, N., Kurvinen, E., and Mikkola, A.: A methodology for product development in mobile machinery: case example of an excavator, Machines, 7, 70, https://doi.org/10.3390/machines7040070, 2019.

Blouin, S., Hemami, A., and Lipsett, M.: Review of resistive force models for earthmoving processes, J. Aerosp. Eng., 14, 102–111,https://doi.org/10.1061/(ASCE)0893-1321(2001)14:3(102), 2001.

Chang, Q., Cheng, G., and Yang, Z.: Lightweight design of hydraulic excavator stick, J. Phys. Conf. Ser., 2760, 012012, https://doi.org/10.1088/1742-6596/2760/1/012012, 2024.

Deb, K., Pratap, A., Agarwal, S., and Meyarivan, T.: A fast and elitist multiobjective genetic algorithm: NSGA-II, IEEE Trans. Evol. Comput., 6, 182–197, https://doi.org/10.1109/4235.996017, 2002.

Han, D., and Zheng, J.: A survey of metamodeling techniques in engineering optimization, J. East China Univ. Sci. Technol. Nat. Sci. Ed., 38, 762–768, 2012.

Huang, C., Tang, L., Peng, P., Zhang, Z., Wang, J., and Pan, Y.: Lightweight optimization design of hydraulic excavator bucket arm based on Altair Inspire, J. Phys. Conf. Ser., 3019, 012021, https://doi.org/10.1088/1742-6596/3019/1/012021, 2025.

Kim, J. W., Jung, S., Kim, J., and Seo, T.: Optimal design of the front linkage of a hydraulic excavator for multi-objective function, J. Mech. Sci. Technol., 28, 3103–3111, https://doi.org/10.1007/s12206-014-0718-x, 2014.

Kroo, I., Altus, S., Braun, R., Gage, P., and Sobieski, I.: Multidisciplinary optimization methods for aircraft preliminary design, in: 5th Symposium on Multidisciplinary Analysis and Optimization, 4325, 1994.

Li, F., Tong, S., and Wang, X.: Dynamic optimization design for working device of hydraulic excavator based on modal analysis, Trans. Chin. Soc. Agric. Mach., 45, 28–36, 2014.

Li, X., Wang, G., Miao, S., and Li, X.: Optimal design of a hydraulic excavator working device based on parallel particle swarm optimization, J. Braz. Soc. Mech. Sci. Eng., 39, 3793–3805, https://doi.org/10.1007/s40430-017-0798-5, 2017.

Liu, Y. X., Huang, H. Z., and Lu, Y.: Reliability evaluation and optimal design of hydraulic excavator working device using integrated optimal machine learning algorithm, J. Mech. Sci. Technol., 39, 3725–3734, 2025.

Lu, Z., Lin, S., Chen, J., Gu, T., and Xie, Y.: A multi-objective collaborative optimization method for the excavator working device to support energy consumption reduction, Energies, 16, 7056, https://doi.org/10.3390/en16207056, 2023.

Maciejewski, J., Jarzębowski, A., and Trąmpczyński, W.: Study on the efficiency of the digging process using the model of excavator bucket, J. Terramech., 40, 221–233, https://doi.org/10.1016/j.jterra.2003.12.003, 2003.

Madan Mohan, B. A., Ur Rahaman, M., Pavan, G., Madhu, R., and Khot, M. B.: Finite element analysis & topolog y optimization of excavator bucket teeth for optimal performance, Mining Technol., 133, 242–254, https://doi.org/10.1177/25726668241270488, 2024.

Qiu, Q., Li, B., and Feng, P.: Optimal design of hydraulic excavator working device based on multiple surrogate models, Adv.

https://doi.org/10.5194/ms-2026-167
Preprint. Discussion started: 7 September 2026

Mech. Eng., 8, 1687814016647947, https://doi.org/10.1177/1687814016647947, 2016.

Ren, Z., Wang, J., Chen, J., Zhang, J., Liu, J., Liang, Y., and Sun, H.: Active-side calculation method for a backhoe hydraulic excavator with incomplete digging resistance in a normal state, Math. Probl. Eng., 2019, 9846305, https://doi.org/10.1155/2019/9846305, 2019.

Solazzi, L., Assi, A., and Ceresoli, F.: Excavator arms: numerical, experimental and new concept design, Compos. Struct., 217, 60–74, https://doi.org/10.1016/j.compstruct.2019.02.096, 2019.

Solazzi, L., Buffoli, A., and Ceresoli, F.: Weight optimization by using both aluminum and composite material on the big excavator, IOP Conf. Ser. Mater. Sci. Eng., 1190, 012010, 2021.

Solazzi, L., Buffoli, A., and Ceresoli, F.: Fatigue evaluation for innovative excavator arms made of composite material, Materials, 15, 7480, https://doi.org/10.3390/ma15217480, 2022.

Tao, J., Ye, H., Hu, G., Xiang, S., Zhang, T., and Zheng, S.: Optimization design of excavator stick based on improved mayfly optimization algorithm, Appl. Sci., 15, 11658, https://doi.org/10.3390/app152111658, 2025.

Wu, J., Zhao, J., Wang, X., and Lin, B.: Multidisciplinary collaborative design optimization of electric shovel working devices, Machines, 12, 520, https://doi.org/10.3390/machines12080520, 2024.

Wu, Y., and Cai, Y.: Lightweight research on excavator working device considering extreme operation modes, Eng. Res. Express, 8, https://doi.org/10.1088/2631-8695/ae3ce6, 2026.

Yu, X., Pang, X., Zou, Z., Zhang, G., Hu, Y., Dong, J., and Song, H.: Lightweight and high-strength design of an excavator bucket under uncertain loading, Math. Probl. Eng., 2019, 3190819, https://doi.org/10.1155/2019/3190819, 2019.

Zhang, H., Ge, X.-B., Li, Y., Shao, X.-D., and Jia, M.-M.: Lightweight design of excavator working device based on automatically generated surrogate model, Sci. Rep., 14, 29756, https://doi.org/10.1038/s41598-024-80882-5, 2024.

Zhou, L., and Wang, Q.: Lightweight design of the working device for a medium hydraulic excavator, Constr. Mach., 53, 96–100, 2022.

Zu, Q., and Bai, M.: Optimization of structural design parameters in BIM using grid search and immune genetic algorithm, Informatica, 49, 161–173, https://doi.org/10.31449/inf.v49i32.8328, 2025.